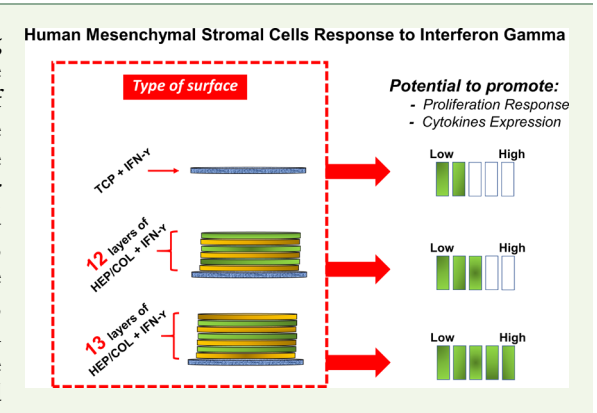


Heparin/Collagen Coatings Improve Human Mesenchymal Stromal Cell Response to Interferon Gamma

David A. Castilla-Casadiego, †,§ José R. García, Andrés J. García, and Jorge Almodovar*, \$\dagger\$.

Supporting Information

ABSTRACT: Mesenchymal stromal cells (MSC) are a promising source for cell-based therapies as they secrete a myriad of reparative factors in response to inflammatory stimuli. In this study, multilayers of heparin and collagen (HEP/COL) were used as a bioactive surface coating to enhance human MSC (hMSC) response to soluble interferon-gamma (IFN- γ). Multilayers were formed, via layer-by-layer assembly, varying the final layer between COL and HEP and supplemented with IFN-γ in the culture medium. hMSC adhesion, proliferation, and cytokine expression were assessed. Infrared variable angle spectroscopic ellipsometry confirmed film chemistry, thickness, and roughness. COL-ending films of 12 layers of HEP/COL had an average thickness of 129 ± 5.8 nm, and 13 layers (HEP-ending) were 178 ± 28.3 nm thick. Changes in temperature between 25–37 °C did not have significant effects on film chemistry, thickness, or roughness.



An EdU incorporation assay revealed that IFN-γ had an antiproliferative effect in all conditions evaluated except when hMSCs were cultured on HEP-ending films supplemented with IFN-γ. Moreover, hMSCs cultured on HEP-ending films supplemented with IFN- γ had a higher cytokine expression as compared with cells cultured on tissue culture polystyrene, COL-ending films with and without IFN- γ , and HEP-ending films without IFN- γ as measured by Luminex assay. Finally, immunostaining revealed strong integrin binding and FAK phosphorylation for each condition. This study shows that HEP/COL films can modulate hMSC response to soluble factors, which may be exploited in cell manufacturing practices.

KEYWORDS: layer-by-layer, human mesenchymal stromal cells, collagen, heparin, interferon gamma, cell manufacturing.

1. INTRODUCTION

The layer-by-layer (LbL) method is a useful strategy to functionalize surfaces of inert materials which are commonly used in the biomedical field. 1,2 Using this technique, it is possible to develop bioactive films or coatings composed of natural or synthetic polymers that provide specific signals to cells, enhancing cellular behavior and potentiating their activities compared to the surface without coating.3 involves sequence-specific electrostatic interactions between polyelectrolytes to produce films with specific and controlled physical-chemical characteristics. 5,6 Our group 6,7 and others⁸⁻¹¹ have shown that LbL film thickness, porosity, wettability, stiffness, and other parameters depend on polymer selection and processing parameters such as solution pH, polymer concentration, and rinsing solution. Moreover, the LbL process can be scaled up and automated, making it an attractive technology from a manufacturing standpoint. 12-14 LbL films are stable when exposed to culture media with or without cells due to the strong electrostatic interactions, although this stability is dependent on polyelectrolyte selection. 15 Through these properties, it is possible to engineer

an active coating capable of providing multiple stimuli for cell culture. LbL films can serve as a platform to present complex surfaces through the functionalization of chemical agents or biochemical signals such as peptides¹⁶ or growth factors,¹⁷ to induce more effective signals by replicating the extracellular environment, enhancing cellular behavior.

The extracellular matrix (ECM) of tissues is composed of a variety of biomacromolecules that includes proteins, glycoproteins, proteoglycans, and polysaccharides. 18 ECM components have been used to develop surfaces or scaffolds that mimic the cellular microenvironment and promote cellular activities for bone cells, 19 cardiac cells, 20 myoblasts, 10 and stem cells,²¹ as potential alternatives for tissue repair or to address degenerative diseases. One of the most relevant proteins to develop scaffolds or surfaces is collagen, which is one of the main components of the ECM of connective tissues.²² Collagen also provides strength and structure to the ECM by

Received: January 2, 2019 Accepted: May 16, 2019 Published: May 16, 2019

Department of Chemical Engineering, University of Puerto Rico Mayaguez, Call Box 9000, Mayaguez, Puerto Rico 00681-9000, United States

^{*}Woodruff School of Mechanical Engineering, Petit Institute for Bioengineering and Bioscience, 315 Ferst Dr., Georgia Institute of Technology, Atlanta, Georgia 30332-0363, United States

directly interacting with cells and other ECM molecules.²³ This protein has demonstrated significant cellular improvements in its different presentations such as nanofibers, 24 sponges, 25,26 and LbL films. 27,28 Likewise, heparin is an essential polysaccharide with multiple contributions at the cellular level. Heparin is a highly sulfated glycosaminoglycan present in the ECM and surface of cells.²⁹ This polysaccharide regulates cell proliferation, cellular adhesion, matrix assembly, migration, immune responses, lipid metabolism, angiogenesis, and wound healing.^{29–31} Proteoglycans of heparan sulfate are also recognized as ubiquitous protein ligands.³⁰ Therefore, their functionality is strongly based on the capacity to recognize diverse proteins which offer a variety of functional properties, from immobilization or protection against proteolytic degradation to different modulations of biological activity.³⁰ Heparin is composed of strong anionic domains enriched with glucosamine N-sulfate and iduronic acid, typically three to eight disaccharides long.³⁰ Collagen and heparin have been used to prepare polymeric multilayers. Their use has been centered on helping promote the blood-compatibility of titanium implants, 2,27,32,33 vascularization studies,³⁴ and intravascular endothelialization with the functionalization of antibodies over the multilayers. 35,36

Interferon gamma (IFN- γ) is a cytokine produced by CD4⁺ lymphocytes and natural killer cells involved in innate and adaptive immunity against viral infections, bacteria, and protozoa.³⁷ Its importance in the immune system lies in its capacity to inhibit viral replication 38-41 and its immunomodulators. 42,43 The active form of this cytokine is a homodimer that consists of two polypeptides of 143 amino acids. 44 IFN-γ binds to heparin, 45 but it does not interact with isolated N-sulfate domains. 30 The dimeric cytokine attaches to an oligosaccharide complex that encompasses an N-acetylated domain rich in glucosamine and two sequences highly sulfated, each one which connects to a monomer of IFN-γ.²⁹ IFN-γ has been used for the treatment and prevention of graft versus host disease, 46 promotes the immunosuppressive capacity of adult human mesenchymal stromal cells (hMSCs),47-49 and promotes the migration of hMSCs in vitro. 50 It also regulates the proliferation and differentiation of MSCs via activation of indoleamine 2,3 dioxygenase.⁵¹

Stem cell manufacturing has emerged as a promising area to generate high-quality cells for many cell-based therapies. 52–54 Studies have demonstrated the clinical potential that stem cells offer to promote advances of new medical applications and therapies for the treatment of diverse diseases and disorders, including Alzheimer's disease, 55 Parkinson's disease, 66 lesions in vertebral disks, 70 diabetes, 88 muscular dystrophy, 99 cancer, 60 myelodysplastic syndromes, 61 autoimmune disorders, 62 and other inflammatory diseases. However, challenges associated with large-scale manufacturing severely limit these therapies. Therefore, there is a need for alternatives to promote the production of stem cells with high therapeutic value, and at the same time, achieve control in reproducibility and cell quality. Increasing the capacity to obtain stem cells with high therapeutic value would eliminate the limiting barrier of a shortage of these cells for the development of treatments that help in the improvement of health and welfare of patients worldwide.

In search of approaches to exert control/improve production of hMSCs, we evaluated hMSCs responses on polymeric multilayers composed of collagen (COL) and heparin (HEP) that are either terminated in COL (12 layers HEP/COL) or

HEP (13 layers HEP/COL) with and without IFN- γ as a supplement in the culture medium. hMSC proliferation, adhesion, and immunomodulatory cytokine expression were evaluated as a function of polymeric multilayer composition in the presence or absence of soluble IFN- γ . Our results show that heparin terminated multilayers negate the antiproliferative effect of IFN- γ while enhancing cytokine expression.

2. MATERIALS AND METHODS

2.1. LbL Film Construction. Heparin sodium (HEP) purchased from Celsius Laboratories, Inc. (cat. no. PH3005) and lyophilized type I collagen sponges (COL) derived from bovine tendon (generously donated by Integra Lifesciences Holdings Corporation, Añasco, PR) were used to prepare polymeric multilayers on sterile tissue culture-treated plates from Corning Costar (cat. no. 07-200-740). The solution used to dissolve the polymers consisted of acetate buffer (0.1 M sodium acetate anhydrous, 0.1 M acetic acid, pH 5), which was also used as the washing solution. All polymeric solutions were prepared at a concentration of 1.0 mg/mL. Ultrapure water at 18 $M\Omega$ ·cm was used to prepare polymeric and wash solutions. In this work, we evaluated layers of HEP/COL ending in COL and HEP constructed using the layer-by-layer technique. The sequence for forming the multilayers consisted in adding poly(ethylenimine) (PEI) (50% solution in Water, Mw \approx 750 000) from Sigma-Aldrich (cat. no. P3143), for 15 min to each well on a 24-well plate. Then HEP and COL were deposited sequentially for 5 min per layer with a 3 min wash in between. The volume of each polymeric solution was 0.6 mL per well. Layers ending in COL were composed of a total of 6 (HEP/ COL) bilayers or 12 layers. Layers ending in HEP were composed of 6.5 (HEP/COL) bilayers or 13 layers. After multilayer preparation, a final wash was performed using DPBS 1× without Ca²⁺ and Mg²⁺. Substrates were sterilized using UV for 15 min.

2.2. Experimental Design. We studied the effects of two factors on cellular response of hMSCs: type of surface and the presence or absence of IFN-γ in the culture medium. The surfaces evaluated were the following: (i) a control surface of tissue culture plastic (TCP), (ii) 12 layers of HEP/COL (layers ending with COL), and (iii) 13 layers of HEP/COL (layers ending with HEP). Conditions with medium supplemented with and without IFN-γ recombinant human protein (ThermoFisher, cat. no. PHC4031) at a concentration of 50 ng/mL were designated as +IFN-γ and –IFN-γ, respectively. A bovine IFN-γ ELISA kit (Invitrogen, cat. no. KBC1231) was used to measure endogenous levels of IFN-γ in the fetal bovine serum used to grow hMSCs (Figure S1).

2.3. Chemical Composition of Multilayers. Infrared variable angle spectroscopic ellipsometry (IR-VASE - Mark II, J.A. Woollam Co. IR-VASE, Lincoln, Nebraska) was used to study the chemistry of the polymeric multilayers constructed over a silicon substrate as described in our previous work on dry films. The chemical composition analysis for all samples was performed in a wavenumber range from $800-1800~{\rm cm}^{-1}$. The measurements were taken using a DTGS detector, an angle of incidence of 70° , a spectral resolution of $16~{\rm cm}^{-1}$, $200~{\rm scans}$ per cycle, 2 cycles, bandwidth of $0.01~\mu{\rm m}$, minimum intensity ratio of 2, sample type as isotropic, zone average polarizer, and single position RCE analyzer.

2.4. Physical Characteristics of Multilayers. The thickness and roughness of the multilayers formed over the silicon substrate were determined using the IRVASE instrument. The WVASE32 software within the IRVASE was used to analyze both properties, as shown in our recent work.⁶ To determine whether exposure of the polymeric multilayers of HEP/COL to a temperature range between 25 and 37 °C exerts significant effects in the physical—chemical properties of the multilayers, a heating stage controlled by an INSTEC—mk2000 coupled to the IRVASE was used to establish controlled heat ramps.

2.5. Cell Culture. hMSCs, from the NIH resource center at Texas A&M Institute for Regenerative Medicine, were used between passages 4–6. hMSCs from a healthy 22-year-old male were used. The product specification sheet provided by the vendor shows that these cells were positive for CD90, CD105, and CD73a hMSCs

ACS Biomaterials Science & Engineering

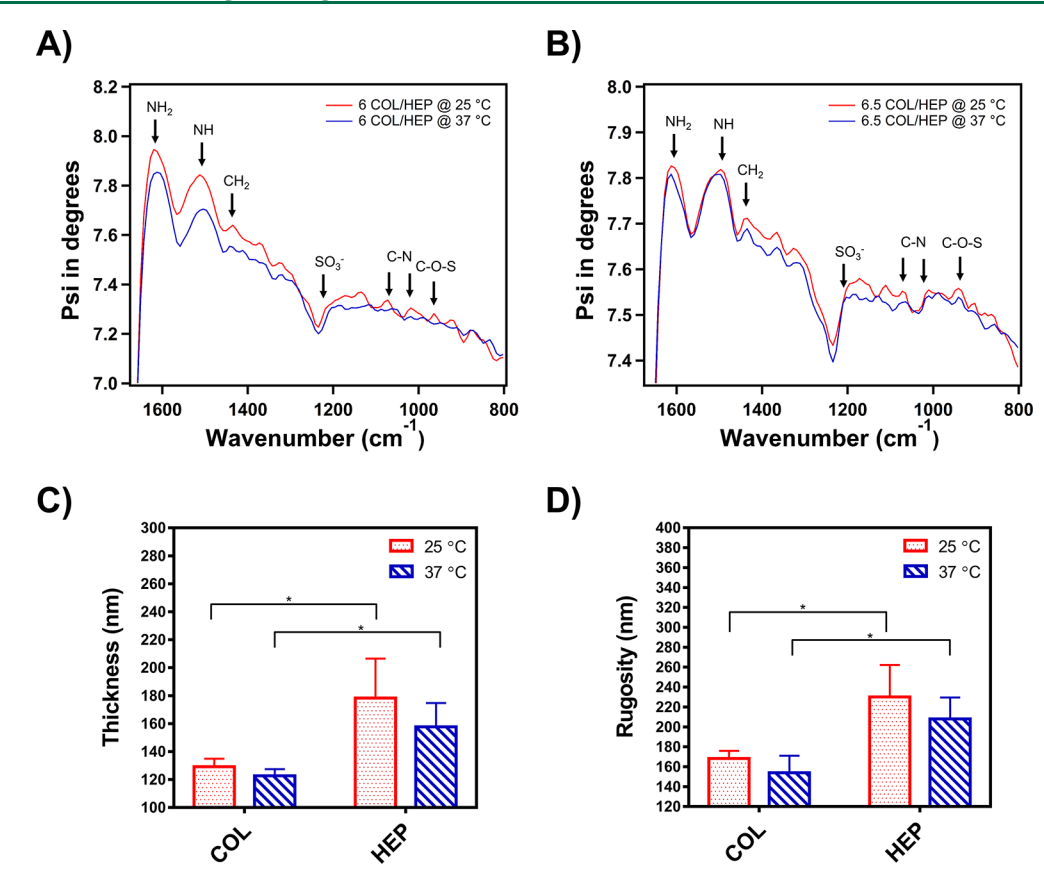


Figure 1. Physical—chemical properties of the multilayers of HEP/COL as measured by IRVASE at 25 and 37 °C. (A) IRVASE Spectrum of 12 layers HEP/COL. (B) IRVASE Spectrum of 13 layers HEP/COL. (C) Thickness vs number of layers (12 and 13 layers). (D) Roughness vs number of layers (12 and 13 layers). Data are presented as the mean \pm standard deviation of n = 4 samples. p < 0.05 are represented by *.

identity markers (as tested by flow cytometry), negative for CD11b, CD45, and CD34 (as tested by flow cytometry), and could differentiate into fat and bone cells. Cells from a second donor and different provider (RoosterBio) were used in a validation experiment (Figure S2). hMSCs were grown in alpha-minimum essential media MEM Alpha (1×) from Gibco (supplemented with L-glutamine, ribonucleosides, and deoxyribonucleosides) (cat. no. 12561-056) containing 20% fetal bovine serum from Gibco (cat. no. 12662029), 1.2% penicillin-streptomycin from Corning (cat. no. 30002CI), and 1.2% L-glutamine from Corning (cat. no. 25005CI).

2.6. Immunofluorescence Staining. Layers of HEP/COL were prepared onto micro coverglass from Electron Microscopy Sciences (cat. no. 72223-01). 6-well plates containing the micro coverglass with and without multilayers were used to culture hMSCs seeded at 10 000 cells/cm².

Immunofluoresence staining for focal adhesions was performed for the detection of the following: phosphorylated FAK (p-FAK) Y397 (Abcam ab81298, source: rabbit, 1:150 dilution) using 488 goat antirabbit secondary antibody (Thermo-Fisher Scientific A11035, 1:200 dilution); beta-1 integrin (DSHB A11B2, source: rat, 1:100 dilution) using 488 goat antirat secondary antibody (R&D systems A11006, 1:100 dilution) and beta-3 integrin (R&D systems AF2266, source: goat, 1:100 dilution) using 488 rabbit antigoat secondary antibody (Life Technologies A11078, 1:100 dilution). AlexaFluor555 Phalloidin (Invitrogen A34055, 1:100 dilution) and DAPI (Invitrogen A34055, 1:1000 dilution) were used in the staining.

For p-FAK staining, samples were washed three times with Dulbecco's phosphate-buffered solution (DPBS), followed by a wash with CSK buffer (10 mM PIPES buffer, 50 mM NaCl, 150 mM sucrose, 3 mM MgCl₂, 1 mM PMSF, 1 μ g/mL leupeptin, 1 μ g/mL aprotinin, 1 μ g/mL pepstatin), then the plates were placed on ice to inhibit protease activity for 1 min. Cell permeabilization and cytoskeleton stabilization consisted of adding ice-cold CSK buffer

with 0.5% Triton X-100 (CSK+) for 1 min with two repetitions. CSK + buffer was aspirated and 4% paraformaldehyde was added and incubated for 30 min at room temperature (RT). Samples were then washed three times with DPBS, and blocked in 33% goat serum for 2 h at 4 °C. The blocking solution was aspirated, and the primary antibody was diluted in 33% goat serum and incubated overnight at 4 °C in humidified dishes. The next day, the primary antibody was recovered and washed three times with DPBS. Samples were counterstained using the secondary antibody, phalloidin, and DAPI, all diluted in 33% goat serum and incubated at RT for 1 h. Lastly, samples were washed three times in DPBS.

For beta-1 and beta-3 integrin staining, the medium was aspirated, and the cells were washed with DPBS and fixed in 4% paraformaldehyde for 15 min at RT. Samples were washed with DPBS and 2 mL of 0.1% Triton X100 was added per coverslip for 10 min at RT. After rinsing in DPBS, samples were blocked in 5% bovine serum albumin (BSA) + 3% goat serum for 1 h at RT. The blocking solution was aspirated, and the primary antibody was diluted in washing buffer (DPBS + 0.5% BSA, 50 mL) and was added and incubated overnight at 4 °C in humidified dishes. The next day, we recovered the primary antibody, and it was washed three times with wash buffer. Secondary antibody, phalloidin, and DAPI were added and incubated at RT for 2 h. Samples were washed three times with wash buffer and then twice with DPBS.

2.7. hMSCs Proliferation Response to HEP/COL Multilayers. For the proliferation assay, a Click-iT Plus EdU Alexa Fluor 488 Imaging Kit from Invitrogen (cat. no. C10337) was used. hMSCs (1400 cells/cm²) were seeded on each surface, and the EdU kit was used after 3 days of culture. The medium was removed, and 10 mM EdU solution was added to the samples. After 18 h, the samples were washed with DPBS without Ca²+ and Mg²+, followed by fixation with 3.7% formaldehyde for 15 min at room temperature. After permeabilization using 0.5% Triton X-100, the samples were

incubated at room temperature for 20 min and washed with 3% BSA twice, the Click-iT reaction cocktail was added, followed by 30 min of incubation and a washing step. For nucleus staining, Hoechst 33342 solution was added for 30 min, followed by extensive washing with DPBS. The samples were visualized using an inverted fluorescence microscope (Eclipse Ti, Nikon, U.S.A.) using a 495/519 nm excitation/emission filters for the Alexa Fluor 488. Images were analyzed using ImageJ software to determine the percentage of EdUpositive nuclei as a measure of proliferation.

2.8. Cytokine Secretion. Cell culture supernatants from hMSCs seeded on TCP and HEP/COL multilayers (10 000 cells/cm²) with and without IFN- γ were collected after 3 days and stored at -80 °C. Human Premixed Multi-Analyte Kit (Magnetic Luminex Assay) from R&D Systems (cat. no. LXSAHM-05) was used to analyze multiple human biomarkers, including interleukin 10 (IL-10), vascular endothelial growth factor (VEGF-A), fibroblast growth factor (FGF-2), colony stimulating factor 1 (M-CSF), and interleukin 6 (IL-6). All reagents were prepared according to the manufacturer's protocol provided. The assay was performed in a flat-bottomed 96-well microplate. 50 μ L of the magnetic microparticle cocktail were added to each well of the microplate. Then 50 μ L of standard or sample (cell culture supernatant prepared to 2-fold dilution) were added per well. The microplate was incubated for 2 h at room temperature (RT) on a horizontal orbital microplate shaker set at 800 \pm 50 rpm. The plate was placed on a magnet that immobilized the magnetic microparticles and allowed for a buffered wash to be performed. Then 50 μ L of the Biotin Antibody Cocktail was added to each well followed by incubation for 1 h at RT on the orbital shaker set at 800 ± 50 rpm. Subsequently, 50 µL of diluted Streptavidin-PE was added to each well after washing, followed by 30 min of incubation at RT on the shaker set at 800 ± 50 rpm. Finally, the microparticles were resuspended by adding of 100 µL of drive fluid to each well. Before reading the plate, it was incubated for 2 min on the shaker, set at 800 ± 50 rpm. Each standard was added in duplicate, and the samples were quintupled. All solutions were protected from light during handling and storage.

The plate was read on a MAGPIX Luminex instrument (Austin, Texas) and analyzed using Millipore Luminex software version 2.0. The analysis software was set to acquire data using 50 μ L of sample per well, to collect a total of 1000 beads with an average of 50 events/bead. The raw data was collected as median fluorescence intensity (MFI). The lower limit of quantification was determined using the lowest standard that was at least 3 times above background. The concentrations of each cytokine were calculated using the MFI and from the standard curve obtained.

2.9. Statistical Analysis. The results are presented as a mean \pm standard error of the mean (SEM). Comparisons among multiple groups for physical—chemical properties studies and cytokine expression for hMSCs on HEP/COL multilayers were performed by two-way analysis of variance (ANOVA). For hMSCs proliferation response to HEP/COL multilayers, a nonparametric test was performed. Graph Pad Prism 7.0 software for Windows was used for statistical analysis. A *p*-value < 0.05 was considered statistically significant.

3. RESULTS AND DISCUSSION

3.1. Chemical and Physical Characteristics of the Bioactive Multilayered Surface. Heparin/Collagen (HEP/COL) multilayers were deposited on silicon substrates composed of 12 and 13 HEP/COL layers. IRVASE was used to confirm film composition/chemistry and determine the thickness and roughness of the films. Figure 1 shows the physical—chemical properties of HEP/COL films evaluated at 25 and 37 °C. The IRVASE spectra for 12 layers HEP/COL (layers ending in COL) and 13 layers HEP/COL (layers ending in HEP) are shown in Figure 1A,B, respectively. Analyses of spectra revealed the presence of the characteristic bands of both polymers, as was described in our recently

published work.⁶ Peaks for collagen and heparin correspond to the amide I (1700–1600 cm⁻¹) and amide II (1600–1500 cm⁻¹) regions, characteristic of both proteins and polysaccharides.⁶ In both spectra, it is also possible to identify other peaks for HEP such as CH₂ scissoring at 1442 cm⁻¹, SO₃⁻ at 1211 cm⁻¹, C–N stretching at 1072 and 1026 cm⁻¹, and the C–O–S stretching vibration at approximately 987 cm⁻¹, as has been described in the literature.⁶

When comparing the spectra presented in Figure 1A,B, we notice a significant difference between the amide I (1700–600 cm⁻¹) and amide II (1600–1500 cm⁻¹). In the spectrum shown in Figure 1B, multilayers terminated in HEP present an increase in the intensity of the corresponding peak of amide II between 1600–1500 cm⁻¹, surpassing the intensity of amide I in 1700–1600 cm⁻¹, in contrast to the spectrum presented in Figure 1A for multilayers terminated in COL.

This difference is related to the fact that the amide II band represents a significant contribution to the heparin spectrum in comparison to amide I. The opposite is true for collagen. The IRVASE and FTIR spectra of collagen and heparin dissolved in acetate buffer reported in our previous work also showed the same results.⁶ Therefore, IRVASE confirmed the characteristic peaks of COL and HEP, which could be observed in the spectra obtained at 25 °C (temperature of fabrication of multilayers) and 37 °C (temperature of cell culture) when using a heating stage. We note that changes in temperature between 25-37 °C do not induce a drastic effect on the chemical composition of multilayers of 12 and 13 layers of HEP/COL consistent with our recent work.⁶ In our previous work, HEP/COL films were constructed using an automated robotic dipping machine.⁶ In this work, the multilayers were assembled manually by immersion of the substrate. Although the films were constructed manually, similar results were obtained thus confirming the LBL construction of HEP/COL

IRVASE analyses indicated an average thickness of 129 \pm 5.8 nm for 12 layers and 178 \pm 28.3 nm for 13 layers at 25 °C (Figure 1C). Heating the multilayers to a controlled temperature of 37 °C, replicating the temperature of cell culture, yielded a reduction in thickness of 5.4% for 12 layers; obtaining a thickness of 122 \pm 4.8 nm. For 13 layers, there was an approximate reduction of 12% over the measurement at 25 °C for a thickness of 157 \pm 17.1 nm. In our previous work, 6 we observed the same trend in thickness reduction with increasing temperature. We attributed this thickness reduction to the heterogeneous charge distribution along the polymeric chain yielding a heterogeneous surface that is more susceptible to temperature changes. This thickness reduction from temperature could also be due to water evaporation from the films. Of note, thickness measurements were performed on dry films.

These films, constructed manually, yielded a larger thickness than those in our previous work constructed using the automated dipping robot. In our earlier work, 12 layers of HEP/COL films built automatically yielded an average thickness of ~90 nm. Results for surface roughness are presented in Figure 1D, obtaining an average of 168 ± 7.8 nm for 12 layers and 230 ± 32.2 nm for 13 layers. These films, constructed manually, yielded a higher roughness value than those in our previous work built using the automated dipping robot. The differences obtained in thickness and roughness are attributed to the robotic dipping machine because it has a more controlled system of immersion in comparison to a manual immersion which was performed in this work. This is

ACS Biomaterials Science & Engineering

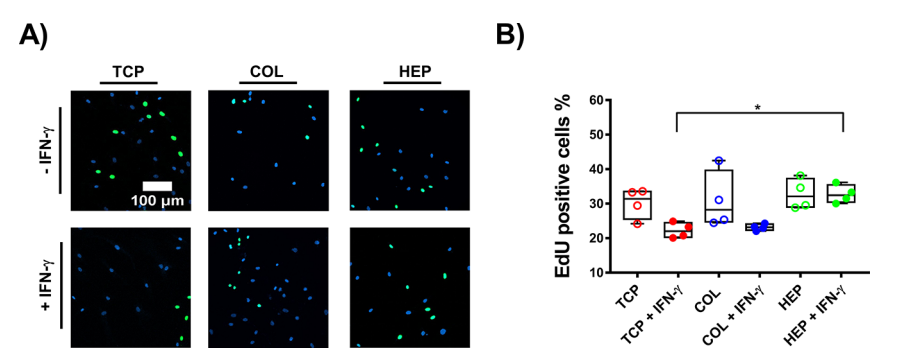


Figure 2. hMSC proliferation response measured by the EdU assay on TCP, 12 layers of HEP/COL (layers ending in COL), and 13 layers of HEP/COL (layers ending in HEP) using medium supplemented with and without IFN- γ . (A) Representative EdU assay images for each condition: the blue color represents the nucleus (DAPI) and the green the EdU label. (B) hMSCs proliferation response. Data are presented as the mean \pm standard deviation of n = 4 samples. The p < 0.05 are represented by *.

because the robotic system maintains a velocity of immersion and extraction constant, which is difficult to control manually. Velocity that can exert an influence over the detachment of the molecules slightly adhered to the substrate, which therefore alters the physical properties of the modified surface. ⁶⁴ We were able to confirm that the changes in temperature between 25-37 °C do not induce a drastic effect on the chemical-physical properties of the polymeric multilayers of HEP/COL, but significant differences (p < 0.05) were observed between multilayers ending in COL and HEP for both physical characterizations of the multilayers (thickness and roughness), as can be observed in Figure 1C,D.

3.2. hMSCs Proliferation Response to HEP/COL Multilayers. An EdU assay was used to measure the proliferation response of hMSCs seeded onto the multilayers of HEP/COL as well as a reference surface—tissue culture polystyrene (TCP). In addition, the effects of IFN- γ in the cell culture media were also evaluated. To test whether the FBS used in the culture media had endogenous IFN- γ , we used an IFN- γ bovine ELISA kit. We observed that the FBS used has undetectable amounts of IFN- γ (Figure S1).

hMSCs were seeded for each experimental condition. The percentage of EdU-positive cells was determined after 18 h of incubation with the EdU solution. Figure 2 summarizes EdU incorporation for hMSCs cultured on COL-ending films, HEP-ending films, and TCP, with (50 ng/mL) or without IFN-γ supplemented in the cell culture media. We selected a concentration 50 ng/mL for soluble IFN-γ based on previous literature⁶⁵ and preliminary experiments. For hMSCs cultured on TCP without IFN-γ, approximately 30% of the cells were EdU-positive. Addition of IFN-γ suppressed proliferation for hMSCs on TCP. This antiproliferative effect for IFN-γ has been reported for multiple cell types, including MSCs. ^{51,66-69}

For films composed of 12 and 13 layers of HEP/COL without IFN- γ , hMSCs displayed equivalent proliferation levels as the TCP reference. Also, significant differences were not observed between multilayers with and without IFN- γ supplement, as can be appreciated in Figure 2A,B.

Our results on the percent of EdU-positive cells for hMSCs seeded over the surfaces supplemented with IFN- γ reported an approximate value of 33%, 23%, and 22% for HEP-terminated films, COL-terminated films, and TCP, respectively (see Figure 2B). HEP-ending layers supplemented with IFN- γ significantly enhanced the proliferation of hMSCs as compared with cells grown on the control TCP surface with IFN- γ supplemented in the culture medium (p < 0.05). Similar

proliferation levels are observed in HEP-ending films with IFN- γ as compared to TCP without IFN- γ . Therefore, HEPending layers might be a suitable surface to preactivate hMSCs in vitro using IFN- γ without affecting their proliferation. IFN- γ activated hMSCs have been shown to exhibit antiviral, antitumor, or immunomodulary properties, which enhance their therapeutic function. ^{69,70} To test the robustness of our technology, we performed a second experiment using hMSCs from a different donor and vendor. hMSCs from a 25-year-old male were obtained from RoosterBio. EdU experiments were performed as described above using the same conditions. We observed that hMSCs from RoosterBio had a high proliferation rate (~70% EdU-positive cells) in conditions without IFN-γ (Figure S2 in Supporting Information). In TCPS, the proliferation rate is greatly reduced to 20% when hMSCs are exposed to 50 ng/mL of IFN-γ. However, hMSCs cultured on COL/HEP films experience a much lower reduction in proliferation, reaching levels of approximately 40%. This confirms that indeed HEP/COL films negate the strong antiproliferative effect of IFN-γ.

Prior studies have reported that heparin is capable of binding with high affinity to a variety of growth factors and cytokines including IFN-7. 71-73 In this work, we did not evaluate the capacity of HEP/COL films to act as a sink for IFN-y. However, previous literature has shown that LbL films of biopolymers do serve as a sink for different growth factors. We have shown that chitosan/heparin LbL films act as a depot for fibroblast growth factors, while poly L-lysine/hyaluronic acid LbL films act as a depot for bone morphogenetic proteins (2 or 7) and stromal derived factor. 74-76 Heparin-binding growth factors strongly bind to heparin-containing films. Nonsulfated glycosaminoglycan also acts as a depot. Given the natural affinity of IFN- γ to heparin, we hypothesize that indeed HEP/ COL films would act as a sink for IFN- γ . Other heparinbinding proteins in the culture media would also be deposited on the films. Our hypothesis regarding the reduced antiproliferative effect of IFN-y when hMSCs are cultured on HEP ending films is due to the natural affinity that IFN-γ binds to both heparan sulfate molecules on the cell membrane and to extracellular heparin.⁷³ It is also known that IFN-γ binds with high affinity to heparan sulfate and heparin molecules through its carboxyl-terminal domain.⁷⁷ Maciag and collaborators reported that heparin helps counteract the antiproliferative effect of IFN-γ on endothelial cells. They demonstrated that IFN-γ inhibited alpha-endothelial cell growth factor and induced endothelial cell proliferation with a simultaneous **ACS Biomaterials Science & Engineering**

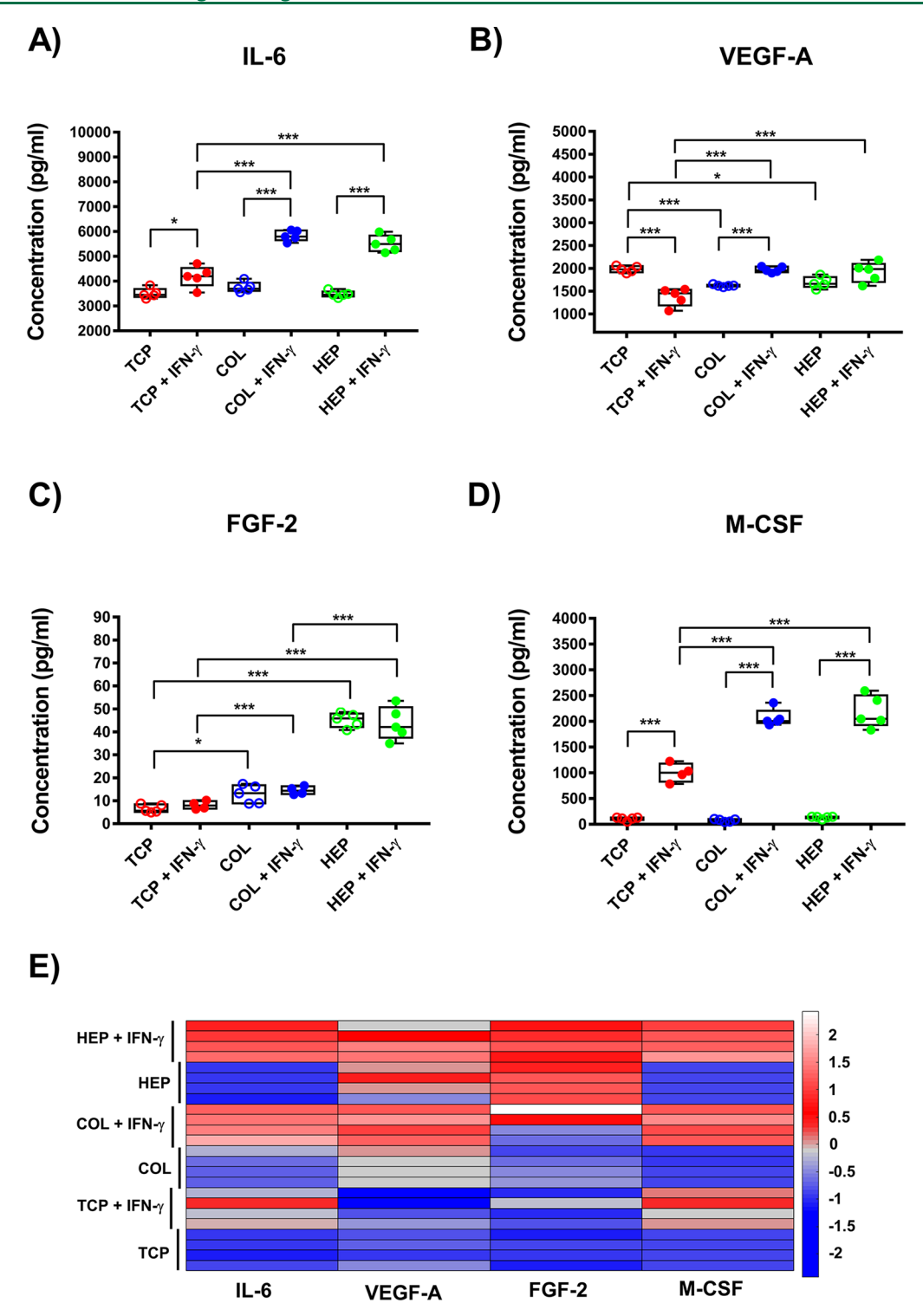


Figure 3. Cytokine levels as assessed by Luminex assay. Comparative protein expression of hMSCs seeded on TCP, 12 layers of HEP/COL (layers ending in COL), and 13 layers of HEP/COL (layers ending in HEP) using medium supplemented with and without IFN- γ . (A) IL-6. (B) VEGF-A. (C) FGF-2. (D) M-CSF. (E) Heatmap representing the concentration values of biomarkers expression individual in each condition evaluated. Blue, low expression: red, high expression. Data are presented as the mean \pm standard deviation of n = 4 samples. The p-values < 0.05 are represented by * and p-values < 0.001 by ***.

change in endothelial cell morphology. However, the addition to the 5 μ g/mL of heparin was able to overcome the antiproliferative effects of IFN- γ partially in the growth of human umbilical vein endothelial cells. This effect is mediated by the inhibition that occurs when cytokines are linked to heparin molecules on the cellular surface. This is due

to the direct competition between linking IFN- γ by soluble heparin and heparin in the cellular surface, failing transduction of the normal receptor signal. 45,79

3.3. Cytokine Expression for hMSCs on HEP/COL Multilayers. A Human Premixed Multi-Analyte Kit (Magnetic Luminex Assay) assay was used for the simultaneous detection

and quantification of multiple human cytokines. We examined IL-6 because of its capacity in regulating proinflammatory and immunoregulatory responses that contribute to the defense of the host against infections and tissue lesions. 80 VEGF-A plays a role in normal physiological functions such as bone formation, hematopoiesis, wound healing, and development.81 FGF-2 controls cellular survival, proliferation, and differentiation.⁸² M-CSF plays an important role in proliferation, differentiation, and survival of monocytes and macrophages. 83 Furthermore, IL-10 potentiates immunoregulation and inflammation.⁸⁴

hMSCs were cultured on TCP and HEP/COL multilayers with and without medium supplemented with IFN-γ (50 ng/ mL). Figure 3 shows results for cytokine expression. A heat map is shown in Figure 3E. IL-10 levels were below the detection levels for all experimental groups.

Our results show that the expression of IL-6 secreted by the hMSCs increases due to the presence of IFN-y for the three different surfaces evaluated. IFN- γ is been known to increase IL-6 secretion in multiple cell types including hMSCs. 85-87 In Figure 3A, we can observe a significant difference in *p*-values < 0.05 between the TCP surface with and without IFN-γ. We observed an increase (p < 0.001) in the expression of IL-6 on both types of multilayers when comparing conditions with and without IFN- γ . Also, we noticed that the multilayers without IFN-γ supplement had a similar IL-6 expression than the TCP surface. Similar results were obtained for M-CSF expression (Figure 3D), where an up-regulation was observed in conditions with soluble IFN-y. In Figure 3D, we see that the expression of M-CSF was upregulated in conditions in which the hMSCs were seeded on the multilayers supplemented with IFN-γ in comparison to the TCP surface supplemented with IFN- γ (p-values < 0.001). IFN- γ has been demonstrated to increase the production and receptor internalization of M-CSF. 88 For VEGF-A (see Figure 3B), we noticed that the addition of IFN-γ causes a decrease in VEGF-A expression for cells cultured on TCP (p-values < 0.001). For cells cultured on HEP/COL films, VEGF-A secretion increases. COL-ending films had a statistically significant (p-values < 0.001) increase in VEGF-A expression when stimulated by IFN- γ. HEPending films showed no statistical difference in VEGF-A secretion when stimulated with IFN- γ . These results suggest the HEP/COL films are enhancing IFN-γ's activity by improving the secretion of IL-6, M-CSF, and VEGF-A. HEP/COL films have the potential to be a suitable surface for producing preactivated hMSCs with a higher immunosuppressive capability than those cultured in TCP with soluble IFN-γ.

Interestingly, FGF-2 expression is unaffected by the presence of IFN-7, but its expression drastically increases on HEPterminated coatings with or without IFN- γ (see Figure 3C). Previous literature suggests that heparin in solution activates the FGF-2 signaling pathway in hMCSs (by phosphorylation of the FGF-2 receptors) and regulates the cell cycle in a dosedependent manner.⁸⁹ Also, we have previously demonstrated that heparin-containing coatings can serve as reservoirs for FGF-2 and that bound FGF-2 modulates MSCs proliferation.⁷⁴ In vitro, FGFs are tightly bound to heparin proteoglycans, which regulates diffusion through the ECM and serve as cofactors that regulate specificity and affinity for the FGF-2 receptor signaling.90 These results suggest that HEP/COL coatings ending in HEP are activating the FGF-2 receptors in hMSCs and thus inducing FGF-2 secretion.

HEP/COL polymeric multilayers are potential platforms for enhancing the preactivation of hMSCs using soluble IFN- γ , as shown by the enhancement in the secretion of key cytokines. Analyzing Figure 3E, which corresponds to the heat map representing the concentration values of biomarker expression in each condition evaluated, we can visually observe that the condition that promotes higher values of expression of these proteins are multilayers ending in HEP with IFN-γ supplemented in the culture medium. Multilayers ending in HEP could be used as a bioactive surface to pretreat hMSCs. This pretreatment could yield more robust and therapeutically relevant hMSCs. That is because HEP-ending layers supplemented with IFN-γ can promote the production of cells with pro-inflammatory and immunoregulatory capacities.

To test the robustness of our technology, we performed a second experiment using hMSCs from a different donor and vendor. hMSCs from a 25-year-old male were obtained from RoosterBio. Luminex experiments were performed as described above using the same conditions. We observed that hMSCs from RoosterBio had a similar response in cytokine expression when exposed to IFN- γ (see Figure S3 in Supporting Information). RoosterBio's hMSCs treated with IFN-γ showed an increase in expression of IL-6 and M-CSF for all the tested conditions. For these cells, expression of IL-6 and M-CSF was unaffected by the presence of the COL/HEP films. Although there are some slight differences in cytokine expression between the different donors, in general we can state that IFN-y enhances immunocytokine expression, and COL/HEP films can boost the effect of IFN-γ on cells that have a low expression of IL-6 and M-CSF. Expression of VEGF was suppressed in the presence of IFN-γ; however, this suppression was decreased by the COL/HEP films specially when terminated in HEP (see Figure S3). Lastly, FGF-2 expression was unaffected by IFN-γ but was significantly enhanced for cells cultured on COL/HEP films (see Figure S3). FGF-2 expression is significantly enhanced by the presence of the COL/HEP films in both donors, in particular on HEP terminated surfaces. This confirms an enhancing effect in hMSCs proliferation by FGF-2 expression.

3.4. Analysis of Cell Adhesive Proteins. Integrins are the principal receptors for components of the extracellular matrix, implicated in cellular adhesion and the regulation of diverse biological processes.^{91,92} Because of the critical role of integrins in modulating cell-material interactions, we examine the assembly of focal adhesions containing beta-1 and beta-3 integrins for hMSCs cultured on TCP and HEP/COL multilayers. Beta-1 and beta-3 integrins are the major subfamilies of integrins involved in cell adhesion to the matrix. In addition, we examined the localization of phosphorylated FAK at tyrosine 397 (p-FAK), an essential kinase regulating integrin signaling and various cell processes, including cell migration, cell spreading, differentiation, survival, gene expression, cytoskeleton protein phosphorylation, apoptosis, and cell cycle progression. 93 Figure 4 presents high magnification images for p-FAK, beta-1, and beta-3 immunostaining as well as phalloidin-labeled actin fibers for hMSCs cultured for 3 days on the different substrates in the presence and absence of IFN-γ. Low power images are presented in Figure S4. In the absence of IFN- γ , cells exhibited well-defined, punctate focal adhesions that stained for p-FAK, beta-1, and beta-3 integrin. In contrast, exposure to IFN-γ resulted in differences in the staining intensity for p-FAK, beta-1, and beta-3 integrin. The reduction in fluorescent intensity for these

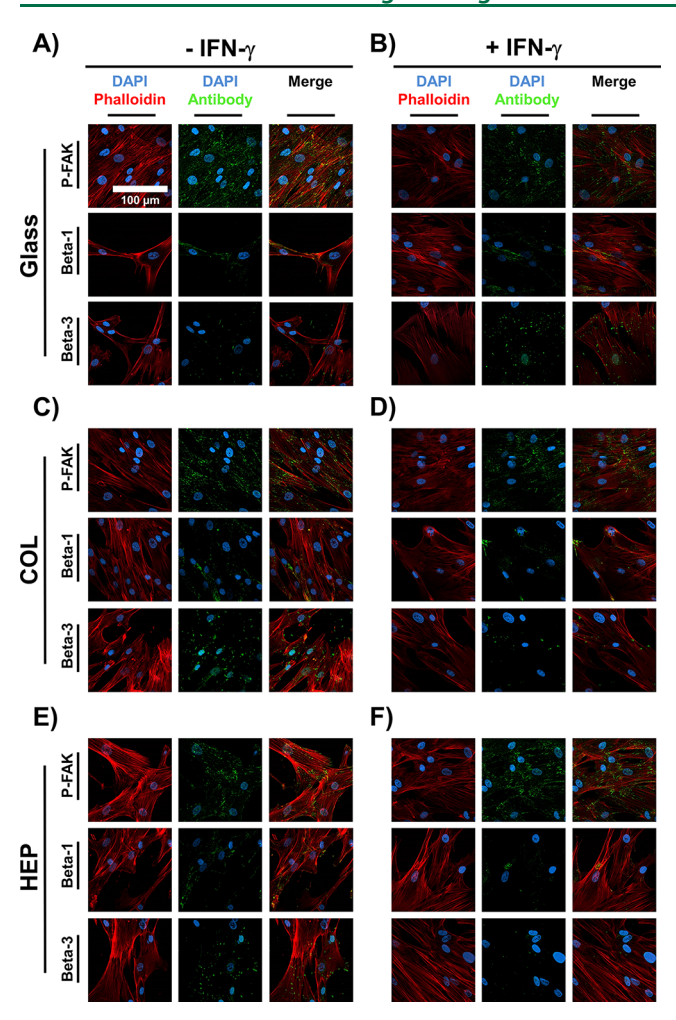


Figure 4. Analysis of hMSCs adhesion after incubation for 3 days. (A) Images of triple staining with phalloidin for actin filaments (red); DAPI for nuclei (blue); and antibodies against p-FAK, Beta-1, and Beta-3 (green) showed focal adhesion formation for hMSCs cultured without IFN-γ. (B) Images of triple staining for hMSCs cultured with IFN-γ supplement. (C) Fluorescent images of triple staining for hMSCs seeded over the surface of 12 layers of HEP/COL without IFN-γ supplement. (D) Fluorescent images of triple staining for hMSCs seeded over the surface of 12 layers of HEP/COL with IFN-γ supplement. (E) Fluorescent images of triple staining for hMSCs seeded over 13 layers of HEP/COL without IFN-γ supplement. (F) Fluorescent images of triple staining for hMSCs seeded over 13 layers of HEP/COL with IFN-γ supplement.

adhesive proteins was observed across all substrates. Despite these significant differences for adhesive proteins, no gross differences in actin cytoskeleton in response to IFN- γ were evident.

4. CONCLUSIONS

A substrate composed of polymeric multilayers of HEP/COL terminating in COL (12 layers HEP/COL) or HEP (13 layers HEP/COL) with IFN- γ supplementation in the culture medium was able to promote the improvement of cellular behaviors of hMSCs, as measured by the ability to proliferate and increase in expression of IL-6, VEGF-A, FGF-2, and M-CSF. hMSCs cultured on HEP/COL multilayers supplemented with IFN- γ demonstrated an enhanced behavior compared to standard TCP. Using these coatings (especially HEP-ending films) allows the preactivation of hMSCs using

IFN-γ to enhance their immunomodulatory properties and therapeutic potential while eliminating IFN- γ 's antiproliferative effect. Our results suggest that this technology could be implemented in hMSC manufacturing by creating surfaces that allow their preactivation without limiting their growth. Future studies will focus on elucidating the mechanisms by which HEP-terminated films enhance IFN-γ activity. Moreover, we will perform experiments to evaluate the translational potential of this technology toward manufacturing by coating bioreactors and evaluating xeno-free media. The demand for potent hMSCs has significantly increased because of an increase in clinical trials in the United States and as a result of cell therapies being approved in Europe, China, and India, 94 which have created large quantities of potent hMSCs. hMSCs therapies have been proposed for the treatment of multiple diseases ranging from neurological disorders to cancer. Typical dose sizes for these treatments are in the order of 10s to 100s of millions of cells per patient. 95 This high dose requirement presents an opportunity to improve cell manufacturing practices, to ultimately reduce patient costs and improve the lives of more patients. Preactivation of hMSCs cultured on HEP-terminated layer-by-layer surfaces may be a solution to produce large quantities of potent hMSCs. The layer-by-layer technology has strong translational potential due to its simplicity, versatility, and scalability, making it attractive to cell manufacturing. This work demonstrates how engineered surfaces may be used complementary to biochemical stimuli to obtain more robust and therapeutically relevant hMSCs.

ASSOCIATED CONTENT

S Supporting Information

The Supporting Information is available free of charge on the ACS Publications website at DOI: 10.1021/acsbiomaterials.9b00008.

Analysis of endogenous IFN-γ levels in the fetal bovine serum is shown, EdU proliferation assay results and Luminex cytokine expression results for hMSCs from RoosterBio, low power images of immunostaining of adhesive proteins of hMSCs for each group after 3 days of incubation by fluorescent detection at 20× (PDF)

AUTHOR INFORMATION

Corresponding Author

*E-mail: jlalmodo@uark.edu.

ORCID ®

Jorge Almodovar: 0000-0002-1151-3878

Present Address

§D.A.C.-C., J.A.: Ralph E. Martin Department of Chemical Engineering, University of Arkansas, 3202 Bell Engineering Center, Fayetteville, AR 72701, Phone: +1 479-575-3924, Fax: +1 479-575-7926.

Notes

The authors declare no competing financial interest.

ACKNOWLEDGMENTS

This work was financially supported by the Engineering Research Center for Cell Manufacturing Technologies (CMaT) of the National Science Foundation under Grant No. EEC-1648035, the Army Research Office under Contract No. W911NF-15-1-0031, and by the "Programa de Apoyo Institucional Para la Formación en Estudios de Posgrados en

Maestrias y Doctorados de La Universidad del Atlántico, Colombia" by providing DCC a scholarship. The authors thank Luis C. Pinzon Herrera for his collaboration in the development of preliminary experiments in the physical—chemical characterization of the HEP/COL multilayers and fruitful discussions. The authors thank Integra LifeSciences for donating the collagen used in this work. The authors thank Dr. Shannon Servoss, Dr. Lauren Greenlee, and Dr. Raj Rao from the University of Arkansas for equipment access and help during the ELISA and second donor testing experiments. The authors declare no financial interest.

REFERENCES

- (1) Shi, J.; Liu, Y.; Wang, Y.; Zhang, J.; Zhao, S.; Yang, G. Biological and immunotoxicity evaluation of antimicrobial peptide-loaded coatings using a layer- by-layer process on titanium. *Sci. Rep.* **2015**, 5, 16336.
- (2) Chen, J.; Chen, C.; Chen, Z.; Chen, J.; Li, Q.; Huang, N. Collagen/heparin coating on titanium surface improves the biocompatibility of titanium applied as a blood-contacting biomaterial. *J. Biomed. Mater. Res., Part A* **2010**, 95A (2), 341–349.
- (3) Tang, B. Z.; Wang, Y.; Podsiadlo, P.; Kotov, N. A. Biomedical Applications of Layer-by-Layer Assembly: From Biomimetics to Tissue Engineering. *Adv. Mater.* **2006**, *18* (24), 3203–3224.
- (4) Gribova, V.; Auzely-Velty, R.; Picart, C. Polyelectrolyte Multilayer Assemblies on Materials Surfaces: From Cell Adhesion to Tissue Engineering. *Chem. Mater.* **2012**, *24* (5), 854–869.
- (5) Crespilho, F. N.; Zucolotto, V.; Oliveira, O. N., Jr; Nart, F. C. Electrochemistry of layer-by-layer films: a review. *Int. J. Electrochem.* **2006**, *1* (5), 194–214.
- (6) Castilla-Casadiego, D. A.; Pinzon-Herrera, L.; Perez-Perez, M.; Quiñones-Colón, B. A.; Suleiman, D.; Almodovar, J. Simultaneous characterization of physical, chemical, and thermal properties of polymeric multilayers using infrared spectroscopic ellipsometry. *Colloids Surf., A* **2018**, *553*, 155–168.
- (7) Almodóvar, J.; Place, L. W.; Gogolski, J.; Erickson, K.; Kipper, M. J. Layer-by-layer assembly of polysaccharide-based polyelectrolyte multilayers: a spectroscopic study of hydrophilicity, composition, and ion pairing. *Biomacromolecules* **2011**, *12* (7), 2755–2765.
- (8) Boddohi, S.; Killingsworth, C. E.; Kipper, M. J. Polyelectrolyte multilayer assembly as a function of pH and ionic strength using the polysaccharides chitosan and heparin. *Biomacromolecules* **2008**, 9 (7), 2021–2028.
- (9) Crouzier, T.; Picart, C. Ion Pairing and Hydration in Polyelectrolyte Multilayer Films Containing Polysaccharides. *Biomacromolecules* **2009**, *10* (2), 433–442.
- (10) Ren, B. K.; Crouzier, T.; Roy, C.; Picart, C. Polyelectrolyte Multilayer Films of Controlled Stiffness Modulate Myoblast Cell Differentiation. *Adv. Funct. Mater.* **2008**, *18* (9), 1378–1389.
- (11) Picart, C. Polyelectrolyte Multilayer Films: From Physico-Chemical Properties to the Control of Cellular Processes. *Curr. Med. Chem.* **2008**, *15* (7), 685–697.
- (12) Krogman, K. C.; Cohen, R. E.; Hammond, P. T.; Rubner, M. F.; Wang, B. N. Industrial-scale spray layer-by-layer assembly for production of biomimetic photonic systems. *Bioinspiration Biomimetics* **2013**, *8* (4), 045005.
- (13) Mateos, A. J.; Cain, A. A.; Grunlan, J. C. Large-Scale Continuous Immersion System for Layer-by-Layer Deposition of Flame Retardant and Conductive Nanocoatings on Fabric. *Ind. Eng. Chem. Res.* **2014**, *53* (15), 6409–6416.
- (14) Machillot, P.; Quintal, C.; Dalonneau, F.; Hermant, L.; Monnot, P.; Matthews, K.; Fitzpatrick, V.; Liu, J.; Pignot-Paintrand, I.; Picart, C. Automated Buildup of Biomimetic Films in Cell Culture Microplates for High-Throughput Screening of Cellular Behaviors. *Adv. Mater.* 2018, 30 (27), 1801097.
- (15) Sergeeva, Y. N.; Huang, T.; Felix, O.; Jung, L.; Tropel, P.; Viville, S.; Decher, G. What is really driving cell-surface interactions? Layer-by-layer assembled films may help to answer questions

- concerning cell attachment and response to biomaterials. Biointerphases 2016, 11 (1), 019009.
- (16) Picart, C.; Elkaim, R.; Richert, L.; Audoin, F.; Arntz, Y.; Da Silva Cardoso, M.; Schaaf, P.; Voegel, J.; Frisch, B. Primary Cell Adhesion on RGD-Functionalized and Covalently Crosslinked Thin Polyelectrolyte Multilayer Films. *Adv. Funct. Mater.* **2005**, *15* (1), 83–94.
- (17) van den Beucken, J. J. J. P.; Walboomers, X. F.; Boerman, O. C.; Vos, M. R.; Sommerdijk, N. A.; Hayakawa, T.; Fukushima, T.; Okahata, Y.; Nolte, R. J.; Jansen, J. A. Functionalization of multilayered DNA-coatings with bone morphogenetic protein 2. *J. Controlled Release* **2006**, *113* (1), 63–72.
- (18) Lu, P.; Weaver, V. M.; Werb, Z. The extracellular matrix: a dynamic niche in cancer progression. *J. Cell Biol.* **2012**, *196* (4), 395–406
- (19) Yang, X. B.; Bhatnagar, R. S.; Li, S.; Oreffo, R. O. C. Biomimetic Collagen Scaffolds for Human Bone Cell Growth. *Tissue Eng.* **2004**, *10* (7–8), 1148–1159.
- (20) Dar, A.; Shachar, M.; Leor, J.; Cohen, S. Cardiac Tissue Engineering Optimization of Cardiac Cell Seeding and Distribution in 3D Porous Alginate Scaffolds. *Biotechnol. Bioeng.* **2002**, 80 (3), 305–312.
- (21) Brunelle, A. R.; Horner, C. B.; Low, K.; Ico, G.; Nam, J. Electrospun thermosensitive hydrogel scaffold for enhanced chondrogenesis of human mesenchymal stem cells. *Acta Biomater.* **2018**, *66*, 166–176.
- (22) Parenteau-Bareil, R.; Gauvin, R.; Berthod, F. Collagen-Based Biomaterials for Tissue Engineering Applications. *Materials* **2010**, 3 (3), 1863–1887.
- (23) Di Lullo, G. a.; Sweeney, S. M.; Körkkö, J.; Ala-Kokko, L.; San Antonio, J. D. Mapping the ligand-binding sites and disease-associated mutations on the most abundant protein in the human, type I collagen. *J. Biol. Chem.* **2002**, *277* (6), 4223–4231.
- (24) Castilla-Casadiego, D. A.; Rivera-Martínez, C. A.; Quiñones-Colón, B. A.; Almodóvar, J. Electrospun Collagen Scaffolds. *Electrospun Biomaterials and Related Technologies* **2017**, 21–55.
- (25) Berthod, F.; Hayek, D.; Damour, O.; Collombel, C. Collagen synthesis by fibroblasts cultured within a collagen sponge. *Biomaterials* 1993, 14 (10), 749–754.
- (26) Zhang, B.; Luo, Q.; Deng, B.; Morita, Y.; Ju, Y.; Song, G. Construction of tendon replacement tissue based on collagen sponge and mesenchymal stem cells by coupled mechano-chemical induction and evaluation of its tendon repair abilities. *Acta Biomater.* **2018**, 74, 247–259.
- (27) Chou, C.-C.; Zeng, H.-J.; Yeh, C.-H. Blood compatibility and adhesion of collagen/heparin multilayers coated on two titanium surfaces by a layer-by- layer technique. *Thin Solid Films* **2013**, *549*, 117–122.
- (28) Glowacki, J.; Mizuno, S. Collagen scaffolds for tissue engineering. *Biopolymers* **2008**, 89 (5), 338–344.
- (29) Sarrazin, S.; Bonnaffé, D.; Lubineau, A.; Lortat-Jacob, H. Heparan sulfate mimicry a synthetic glycoconjugate that recognizes the heparin binding domain of interferon-γ inhibits the cytokine. *J. Biol. Chem.* **2005**, 280 (45), 37558–37564.
- (30) Lindahl, U.; Kusche-Gullberg, M.; Kjellen, L. Regulated Diversity of Heparan Sulfate. *J. Biol. Chem.* **1998**, 273 (39), 24979–24982.
- (31) Bernfield, M.; Götte, M.; Park, P. W.; Reizes, O.; Fitzgerald, M. L.; Lincecum, J.; Zako, M. Functions of cell surface heparan sulfate proteoglycans. *Annu. Rev. Biochem.* **1999**, *68* (1), 729–777.
- (32) Chen, J. L.; Li, Q. L.; Chen, J. Y.; Chen, C.; Huang, N. Improving blood-compatibility of titanium by coating collagen heparin multilayers. *Appl. Surf. Sci.* **2009**, 255 (15), 6894–6900.
- (33) Chen, J.; Huang, N.; Li, Q.; Chu, C. H.; Li, J.; Maitz, M. F. The effect of electrostatic heparin/collagen layer-by-layer coating degradation on the biocompatibility. *Appl. Surf. Sci.* **2016**, *362*, 281–289.
- (34) Jin, K.; Ye, X.; Li, S.; Li, B.; Zhang, C.; Gao, C.; Ye, J. A biomimetic collagen/heparin multi-layered porous hydroxyapatite orbital implant for in vivo vascularization studies on the chicken

- chorioallantoic membrane. Graefe's Arch. Clin. Exp. Ophthalmol. 2016, 254 (1), 83–89.
- (35) Lin, Q.; Ding, X.; Qiu, F.; Song, X.; Fu, G.; Ji, J. Biomaterials In situ endothelialization of intravascular stents coated with an anti-CD34 antibody functionalized heparin collagen multilayer. *Biomaterials* **2010**, *31* (14), 4017–4025.
- (36) Lu, S.; Zhang, P.; Sun, X.; Gong, F.; Yang, S.; Shen, L.; Huang, Z.; Wang, C. Synthetic ePTFE Grafts Coated with an Anti-CD133 Antibody- Functionalized Heparin/Collagen Multilayer with Rapid in vivo Endothelialization Properties. *ACS Appl. Mater. Interfaces* **2013**, 5 (15), 7360–7369.
- (37) Ijzermans, J. N. M.; Marquet, R. L. Interferon-gamma: A Review. *Immunobiology* **1989**, *179* (4–5), 456–473.
- (38) De-Simone, F. I.; Sariyer, R.; Otalora, Y.; Yarandi, S.; Craigie, M.; Gordon, J.; Sariyer, I. K. IFN-Gamma Inhibits JC Virus Replication in Glial Cells by Suppressing T-Antigen Expression. *PLoS One* **2015**, *10* (6), e0129694.
- (39) Kokordelis, P.; Kramer, B.; Korner, C.; Boesecke, C.; Voigt, E.; Ingiliz, P.; Glassner, A.; Eisenhardt, M.; Wolter, F.; Kaczmarek, D.; Nischalke, H. D.; Rockstroh, J. K.; Spengler, U.; Nattermann, J. An Effective Interferon-Gamma-Mediated Inhibition of Hepatitis C Virus Replication by Natural Killer Cells Is Associated With Spontaneous Clearance of Acute Hepatitis C in Human Immunodeficiency Virus-Positive Patients. *Hepatology* **2014**, *59* (3), 814–827.
- (40) Abend, J. R.; Low, J. A.; Imperiale, M. J. Inhibitory Effect of Gamma Interferon on BK Virus Gene Expression and Replication. *J. Virol.* **2007**, *81* (1), 272–279.
- (41) Schoenborn, J. R.; Wilson, C. B. Regulation of Interferon- g During Innate and Adaptive Immune Responses. *Adv. Immunol.* **2007**, 96, 41–101.
- (42) Urba, W. J.; Kopp, W. C.; Clark, J. W.; Smith, J. W.; Steis, R. G.; Huber, C.; Coggin, D.; Longo, D. L. The in vivo immunomodulatory effects of recombinant interferon gamma plus recombinant tumor necrosis factor-alfa. *J. Clin. Oncol.* **1991**, *9* (10), 1831–1839.
- (43) Jurado, A.; Carballido, J.; Griffel, H.; Hochkeppel, H. K.; Wetzel, G. D. The immunomodulatory effects of interferon-gamma on mature B-lymphocyte responses. *Experientia* **1989**, *45* (6), 521–526.
- (44) Sadir, R.; Forest, E.; Lortat-jacob, H. The heparan sulfate binding sequence of interferon-γ increased the on rate of the interferon-γ-interferon-γ receptor complex formation. *J. Biol. Chem.* **1998**, 273 (18), 10919–10925.
- (45) Lortat-Jacob, H.; Kleinman, H. K.; Grimaud, J. High-Affinity Binding of Interferon-ey to a Basement Membrane Complex (Matrigel). *J. Clin. Invest.* **1991**, *87*, 878–883.
- (46) Polchert, D.; Sobinsky, J.; Douglas, G. W.; Kidd, M.; Moadsiri, A.; Reina, E.; Genrich, K.; Mehrotra, S.; Setty, S.; Smith, B.; Bartholomew, A. IFN-γ activation of mesenchymal stem cells for treatment and prevention of graft versus host disease. *Eur. J. Immunol.* **2008**, 38 (6), 1745–1755.
- (47) Ryan, J. M.; Barry, F.; Murphy, J. M.; Mahon, B. P. Interferon-g does not break, but promotes the immunosuppressive capacity of adult human mesenchymal stem cells. *Clin. Exp. Immunol.* **2007**, *149* (2), 353–363.
- (48) Sivanathan, K. N.; Gronthos, S. Interferon-Gamma Modification of Mesenchymal Stem Cells: Implications of Autologous and Allogeneic Mesenchymal Stem Cell Therapy in Allotransplantation. *Stem Cell Rev. Reports* **2014**, *10* (3), 351–375.
- (49) Klinker, M. W.; Marklein, R. A.; Lo, J. L.; Wei, C.; Bauer, S. R. Morphological features of IFN- γ stimulated mesenchymal stromal cells predict overall immunosuppressive capacity. *Proc. Natl. Acad. Sci. U. S. A.* **2017**, *114* (13), E2598–E2607.
- (50) Strojny, C.; Boyle, M.; Bartholomew, A. Interferon Gamma treated Dental Pulp Stem Cells Promote Human Mesenchymal Stem Cell Migration In Vitro. *J. Endod.* **2015**, 41 (8), 1259–1264.
- (51) Croitoru-Lamoury, J.; Lamoury, F. M.; Caristo, M.; Suzuki, K.; Walker, D.; Takikawa, O.; Taylor, R.; Brew, B. J. Interferon-γ regulates the proliferation and differentiation of mesenchymal stem

- cells via activation of indoleamine 2, 3 dioxygenase (IDO). *PLoS One* **2011**, 6 (2), e14698.
- (52) Stem Cell Manufacturing; Cabral, J. M. S., de Silva, C. L., Chase, L. G., Diogo, M. M., Eds.; Elsevier, 2016.
- (53) Ding, D. C.; Chang, Y. H.; Shyu, W. C.; Lin, S. Z. Review Human Umbilical Cord Mesenchymal Stem Cells: A New Era for Stem Cell Therapy. *Cell Transplant* **2015**, 24 (3), 339–347.
- (54) Passweg, J. R.; Baldomero, H.; Bader, P.; Bonini, C.; Cesaro, S.; Dreger, P.; Duarte, R. F.; Dufour, C.; Kuball, J.; Farge-Bancel, D.; Gennery, A.; Kroger, N.; Nagler, A.; Sureda, A.; Mohty, M. Hematopoietic stem cell transplantation in Europe 2014: more than 40 000 transplants annually. *Bone Marrow Transplant.* 2016, 51 (6), 786.
- (55) Turgeman, G. The therapeutic potential of mesenchymal stem cells in Alzheimer's disease: converging mechanisms. *Neural Regener. Res.* **2015**, *10* (5), 698–699.
- (56) Teixeira, F. G.; Carvalho, M. M.; Panchalingam, K. M.; Rodrigues, A. J.; Mendes-Pinheiro, B.; Anjo, S.; Manadas, B.; Behie, L. A.; Sousa, N.; Salgado, A. J. Impact of the secretome of human mesenchymal stem cells on brain structure and animal behavior in a rat model of Parkinson's disease. *Stem Cells Transl. Med.* **2017**, *6* (2), 634–346.
- (57) Wei, A.; Shen, B.; Williams, L.; Diwan, A. Mesenchymal stem cells: potential application in intervertebral disc regeneration. *Transl. Pediatr.* **2014**, 3 (2), 71–90.
- (58) Pileggi, A. Mesenchymal Stem Cells for the Treatment of Diabetes. *Diabetes* **2012**, *61* (6), 1355–1356.
- (59) Markert, C. D.; Atala, A.; Cann, J. K.; Christ, G.; Furth, M.; Ambrosio, F.; Childers, M. K. Clinical Review: Current Concepts Mesenchymal Stem Cells: Emerging Therapy for Duchenne Muscular Dystrophy. *PMRJ.* **2009**, *1* (6), 547–559.
- (60) Shah, K. Mesenchymal stem cells engineered for cancer therapy. Adv. Drug Delivery Rev. 2012, 64 (8), 739-748.
- (61) Wang, J.; Xiao, Z. Mesenchymal stem cells in pathogenesis of myelodysplastic syndromes. Stem cell Investig. 2014, 1 (16), 16–19.
- (62) Munir, H.; McGettrick, H. M. Mesenchymal stem cells therapy for autoimmune disease: risks and rewards. *Stem Cells Dev.* **2015**, 24 (18), 2091–2100.
- (63) Newman, R. E.; Yoo, D.; Leroux, M. A.; Danilkovitch-Miagkova, A. *Inflammation Allergy: Drug Targets* **2009**, 8 (2), 110–123.
- (64) Scriven, L. E. Physics and applications of dip coating and spin coating. MRS Online Proc. Libr. 1988, 121, 717–729.
- (65) Wobma, H. M.; Tamargo, M. A.; Goeta, S.; Brown, L. M.; Duran-Struuck, R.; Vunjak-Novakovic, G. The influence of hypoxia and IFN-g on the proteome and metabolome of therapeutic mesenchymal stem cells. *Biomaterials* **2018**, *167*, 226–234.
- (66) Maher, S. G.; Romero-Weaver, A. L.; Scarzello, A. J.; Gamero, A. M. Interferon: Cellular Executioner or White Knight? *Curr. Med. Chem.* **2007**, *14* (12), 1279–1289.
- (67) Borsellino, N.; Crescimanno, M.; Flandina, C.; Leonardi, V.; Rausa L, D. N. Antiproliferative and chemomodulatory effects of interferon-gamma on doxorubicin-sensitive and -resistant tumor cell lines. *Anticancer. Drugs* 1993, 4, 265–272.
- (68) Gajewski, T. F.; Goldwasser, E.; Fitch, F. W. Anti-proliferative effect of IFN-gamma in immune regulation. II. IFN-gamma inhibits the proliferation of murine bone marrow cells stimulated with IL-3, IL-4, or granulocyte-macrophage colony-stimulating factor. *J. Immunol.* 1988, 141 (8), 2635–2642.
- (69) Wall, L.; Burke, F.; Smyth, J. F.; Balkwill, F. The Anti-proliferative Activity of Interferon-γ on Ovarian Cancer: In Vitro and in Vivo. *Gynecol. Oncol.* **2003**, 88 (1), S149–S151.
- (70) Lortat-Jacob, H.; Esterre, P.; Grimaud, J. A. Interferon-gamma, an anti-fibrogenic cytokine which binds to heparan sulfate. *Pathol., Res. Pract.* **1994**, *190* (9–10), 920–922.
- (71) Lindahl, U.; Lidholt, K.; Spillmann, D.; Kjellén, L. More to "heparin" than anticoagulation. *Thromb. Res.* **1994**, 75 (1), 1–32.
- (72) Bashkin, P.; Doctrow, S.; Klagsbrun, M.; Svahn, C. M.; Folkman, J.; Vlodavsky, I. Basic fibroblast growth-factor binds to

- subendothelial extracellular-matrix and is released by heparitinase and heparin-like molecules. *Biochemistry* **1989**, 28 (4), 1737–1743.
- (73) Fritchley, S. J.; Kirby, J. A.; Ali, S. The antagonism of interferon-gamma (IFN- γ) by heparin: examination of the blockade of class II MHC antigen and heat shock protein-70 expression. *Clin. Exp. Immunol.* **2000**, 120 (2), 247–252.
- (74) Almodóvar, J.; Bacon, S.; Gogolski, J.; Kisiday, J. D.; Kipper, M. J. Polysaccharide-based polyelectrolyte multilayer surface coatings can enhance mesenchymal stem cell response to adsorbed growth factors. *Biomacromolecules* **2010**, *11* (10), 2629–2639.
- (75) Almodóvar, J.; Guillot, R.; Monge, C.; Vollaire, J.; Selimovic, Š.; Luc-Coll, J.; Khademhosseini, A.; Picart, C. Spatial patterning of BMP-2 and BMP-7 on biopolymeric films and the guidance of muscle cell fate. *Biomaterials* **2014**, *35* (13), 3975–3985.
- (76) Dalonneau, F.; Lui, X. Q.; Sadir, R.; Almodóvar, J.; Mertani, H. C.; Bruckert, F.; Albiges-Rizo, C.; Weidenhaupt, M.; Lortat-Jacob, H.; Picart, C. The effect of delivering the chemokine SDF-1 in a matrix-bound manner on myogenesis. *Biomaterials* **2014**, *35* (15), 4525–4535.
- (77) Lortat-Jacob, H.; Baltzer, F.; Grimaud, J. A. Heparin decreases the blood clearance of interferon-gamma and increases its activity by limiting the processing of its carboxyl-terminal sequence. *J. Biol. Chem.* **1996**, *271* (27), 16139–16143.
- (78) Friesel, R.; Komoriya, A.; Maciag, T. Inhibition of Endothelial Cell Proliferation by Gamma-Interferon. *J. Cell Biol.* **1987**, *104* (3), 689–696.
- (79) Fritchley, S. J.; Kirby, J. A.; Ali, S. The antagonism of interferon-gamma (IFN-g) by heparin: examination of the blockade of class II MHC antigen and heat shock protein-70 expression. *Clin. Exp. Immunol.* **2000**, *120* (2), 247–252.
- (80) Kishimoto, T.; Tanaka, T. Interleukin 6. Encyclopedia of Inflammatory Diseases 2014, 1–8.
- (81) Duffy, A. M.; Bouchier-Hayes, D. J.; Harmey, J. H. Vascular Endothelial Growth Factor (VEGF) and Its Role in Non-Endothelial Cells: Autocrine Signalling by VEGF. VEGF Cancer 2004, 133–144.
- (82) Ahn, H. J.; Lee, W. J.; Kwack, K.; Do Kwon, Y. FGF2 stimulates the proliferation of human mesenchymal stem cells through the transient activation of JNK signaling. *FEBS Lett.* **2009**, 583 (17), 2922–2926.
- (83) Stanley, E. R.; Berg, K. L.; Einstein, D. B.; Lee, P. S. W.; Pixley, F. J.; Wang, Y. U. N.; Yeung, Y. Biology and Action of Colony Stimulating Factor-1. *Mol. Reprod. Dev.* **1997**, *46* (1), 4–10.
- (84) Nakajima, M.; Nito, C.; Sowa, K.; Suda, S.; Nishiyama, Y.; Nakamura-Takahashi, A.; Nitahara-Kasahara, Y.; Imagawa, K.; Hirato, T.; Ueda, M.; et al. Mesenchymal Stem Cells Overexpressing Interleukin-10 Promote Neuroprotection in Experimental Acute Ischemic Stroke. *Mol. Ther.–Methods Clin. Dev.* **2017**, *6*, 102–111.
- (85) Faggioli, L.; Merola, M.; Hiscott, J.; Furia, A.; Monese, R.; Tovey, M.; Palmieri, M. Molecular mechanisms regulating induction of interleukin-6 gene transcription by interferon-y. *Eur. J. Immunol.* **1997**, 27 (11), 3022–3030.
- (86) Hotfilder, M.; Knupfer, H.; Mohlenkamp, G.; Pennekamp, P.; Knupfers, M.; Van Gool S, W. J. Interferon-gamma increases IL-6 production in human glioblastoma cell lines. *Anticancer Res.* **2000**, *20* (6B), 4445–4450.
- (87) Chinnadurai, R.; Rajan, D.; Qayed, M.; Arafat, D.; Garcia, M.; Liu, Y.; Kugathasan, S.; Anderson, L. J.; Gibson, G.; Galipeau, J. Potency Analysis of Mesenchymal Stromal Cells Using a Combinatorial Assay Matrix Approach. *Cell Rep.* **2018**, 22 (9), 2504–2517.
- (88) Delneste, Y.; Charbonnier, P.; Herbault, N.; Magistrelli, G.; Caron, G.; Bonnefoy, J. Y.; Jeannin, P. Interferon-γ switches monocyte differentiation from dendritic cells to macrophages. *Blood* **2003**, *101* (1), 143–150.
- (89) Furue, M. K.; Na, J.; Jackson, J. P.; Okamoto, T.; Jones, M.; Baker, D.; Hata, R.-I.; Moore, H. D.; Sato, J. D.; Andrews, P. W. Heparin promotes the growth of human embryonic stem cells in a defined serum-free medium. *Proc. Natl. Acad. Sci. U. S. A.* **2008**, *105* (36), 13409–13414.

- (90) Ornitz, D. M.; Itoh, N. The fibroblast growth factor signaling pathway. Wiley Interdiscip. Rev. Dev. Biol. 2015, 4 (3), 215–266.
- (91) Haas, T. A.; Plow, E. F. Integrin-ligarid interactions: a year in review. Curr. Opin. Cell Biol. 1994, 6 (5), 656-662.
- (92) Guan, J. L. Role of focal adhesion kinase in integrin signaling. *Int. J. Biochem. Cell Biol.* **1997**, 29 (8–9), 1085–1096.
- (93) Schlaepfer, D. D.; Hou, S.; Lim, S. T.; Tomar, A.; Yu, H.; Lim, Y.; Mitra, S. K. Tumor necrosis factor- α stimulates focal adhesion kinase activity required for mitogen-activated kinase-associated interleukin 6 expression. *I. Biol. Chem.* **2007**, 282 (24), 17450–17459.
- (94) Robb, K. P.; Fitzgerald, J. C.; Barry, F.; Viswanathan, S. Mesenchymal stromal cell therapy: progress in manufacturing and assessments of potency. *Cytotherapy* **2019**, *21* (3), 289–306.
- (95) Olsen, T. R.; Ng, K. S.; Lock, L. T.; Ahsan, T.; Rowley, J. A. Peak MSC—Are We There Yet? Front. Med. 2018, 5 (178), 14.